Automatic, robust and efficient pole location for planar, uniaxial multilayers

K. A. Michalski

2006/06/12

Geometry

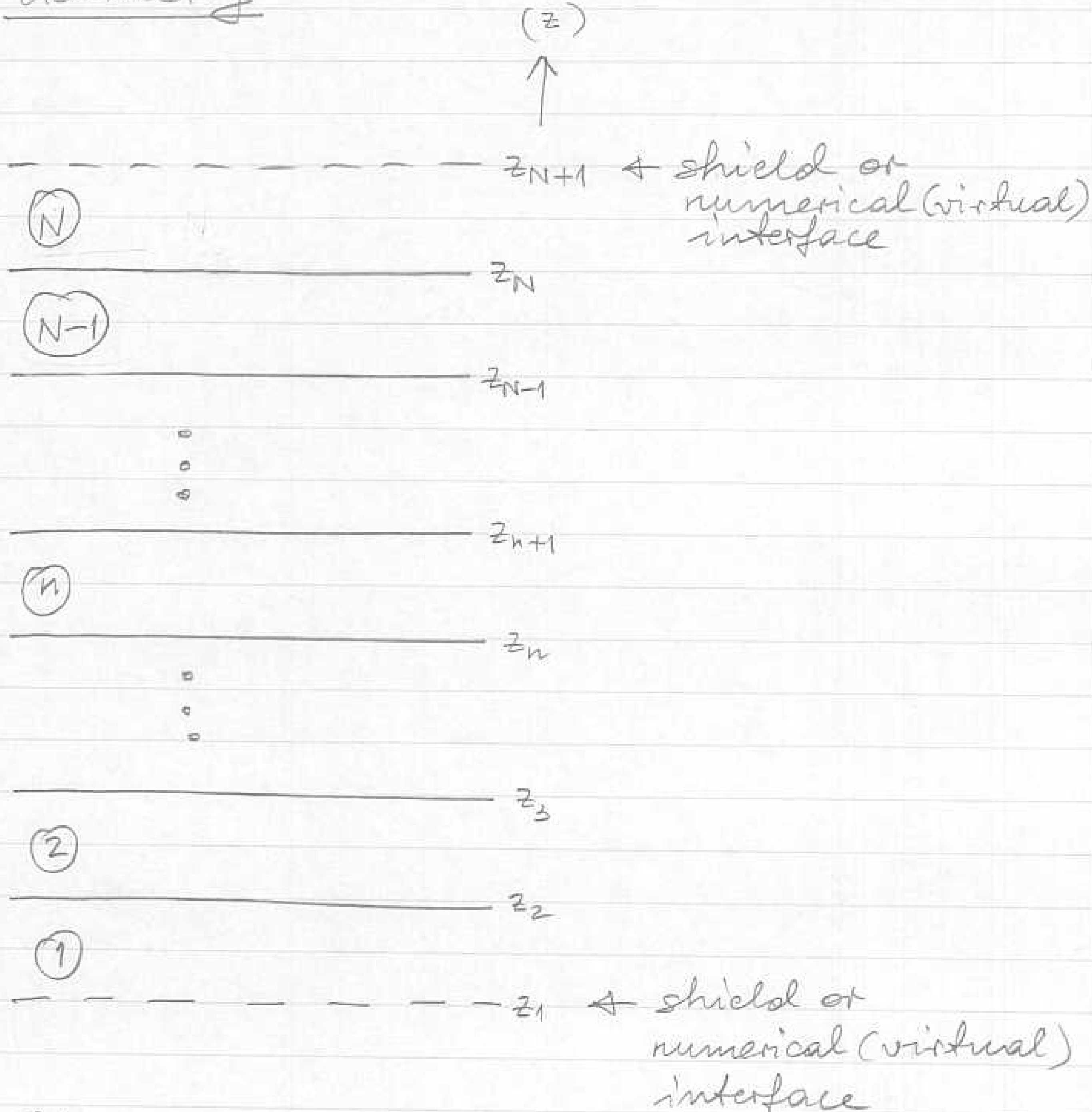

Shield may be PEC, PMC, or surface impedance plane with Z_s specified.

N is assumed to be ≥ 2, unless the medium is shielded below and above, in which case $N=1$ is allowed. There is no upper limit on N.

Examples of geometries that can be handled:

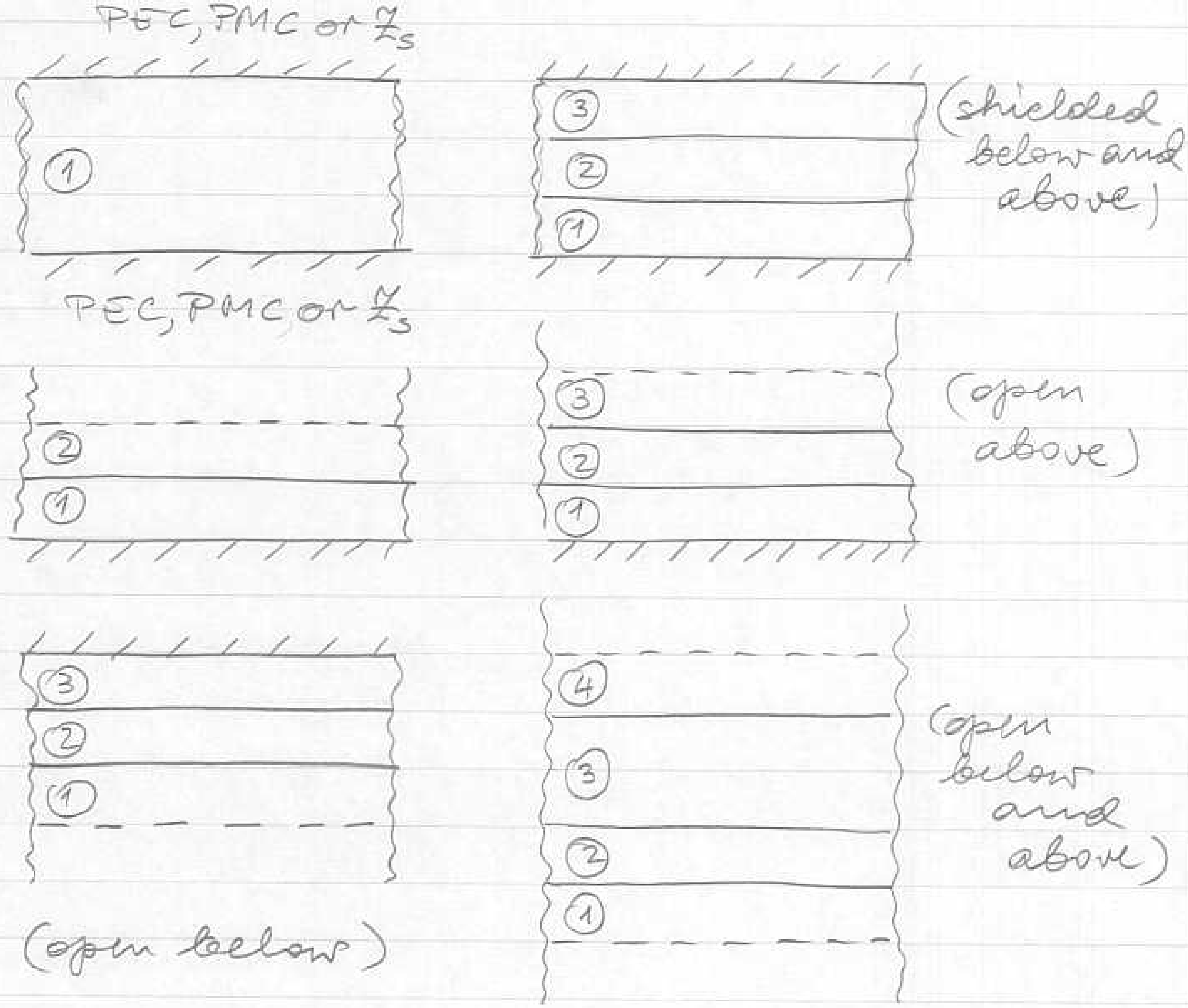

(- - - - are virtual interfaces)

The material of layer n is characterized by (relative to free space)

$$\epsilon_{tn}, \epsilon_{zn}, \mu_{tn}, \mu_{zn}$$

which are complex, in general, with negative imaginary parts. The anisotropy ratios are defined as

$$\nu_n^e = \frac{\epsilon_{zn}}{\epsilon_{tn}}, \quad \nu_n^h = \frac{\mu_{zn}}{\mu_{tn}}$$

which are also in general complex, exept when layer n is a half-space, in which case ν_n^e and ν_n^h must be real.

Two related auxiliary parameters are

$$\lambda_n^\alpha = \sqrt{\nu_n^\alpha} \qquad \alpha = e, h$$

The $e^{j\omega t}$ time convention is assumed.

Upon Fourier transforming the Maxwell's equations w.r.t. the transverse coordinates, a transmission line (TL) analog of the multilayer is obtained.

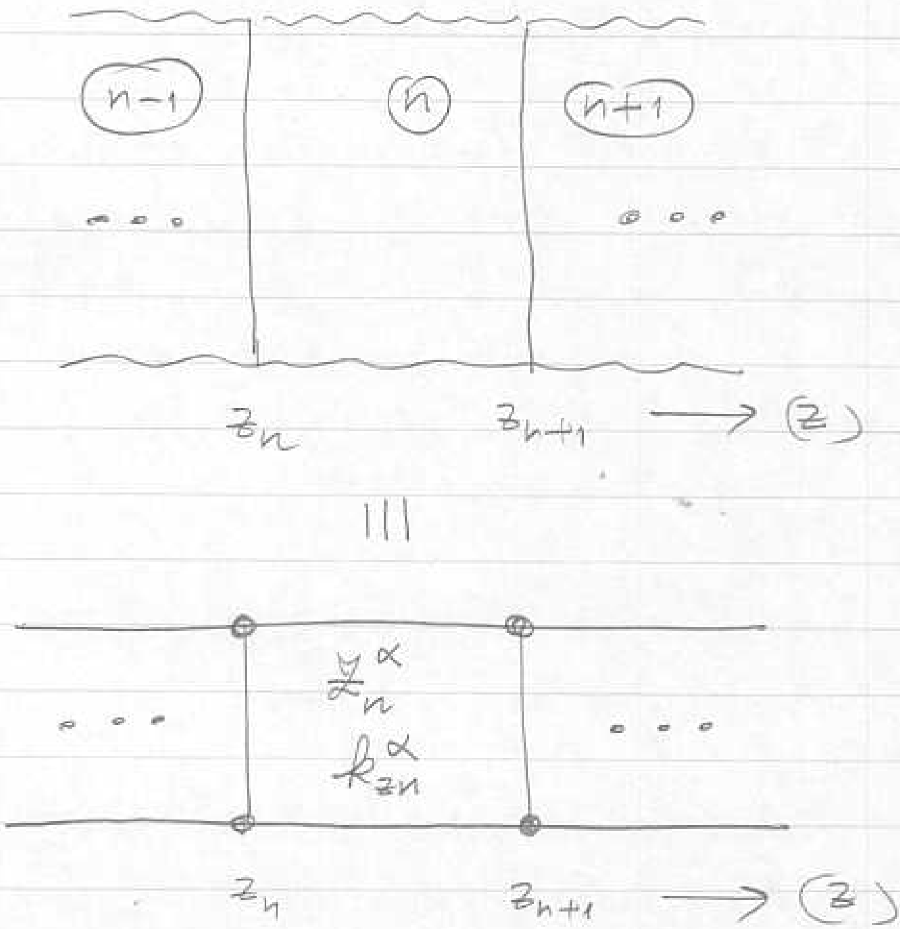

$$\alpha = e, h$$

$$k_{zn}^\alpha = \sqrt{k_n^2 - k_\rho^2/\nu_n^\alpha}, \quad k_n = k_0\sqrt{\epsilon_{tn}\mu_{tn}}$$

$$Z_n^e = \frac{k_{zn}^e}{\omega\epsilon_0\epsilon_{tn}}, \quad Z_n^h = \frac{\omega\mu_0\mu_{tn}}{k_{zn}^h}$$

(Subscript 0 is used to denote free space quantities.)

k_ρ is the transverse wavenumber

The "effective wavenumber" of layer n is

$$k_{eff,n}^{\alpha} = \lambda_n^{\alpha} k_n = \begin{cases} k_0 \sqrt{\epsilon_{zn}\mu_{tn}}, & \alpha = e \\ k_0 \sqrt{\epsilon_{tn}\mu_{zn}}, & \alpha = h \end{cases}$$

The quantities with superscripts "e" and "h" are associated with the TM and TE waves, respectively.

When k_n, k_{effn}^{α}, and k_{zn}^{α} are computed square roots with non-positive imaginary parts are selected; if the imaginary part is zero the square root branch with positive real part is selected.

In the above,

$$k_0 = \omega \sqrt{\mu_0 \epsilon_0}$$

The spectral domain electric and magnetic fields in the multi-layer may be expressed in terms of the voltages and currents on the TL analog. The TM ($\alpha = e$) and TE ($\alpha = h$) TL networks can be analyzed separately.

We omit the superscript α if there is no danger of confusion.

The voltage and current on nth TL section (corresponding to nth layer) can be expressed as

$$\begin{cases} V_n(z) = V_n^+ \, e^{-jk_{zn}(z-z_n)} + V_n^- \, e^{+jk_{zn}(z-z_n)} \\ I_n(z) = \dfrac{V_n^+}{Z_n} e^{-jk_{zn}(z-z_n)} - \dfrac{V_n^-}{Z_n} e^{+jk_{zn}(z-z_n)} \end{cases} \quad (1)$$

Alternatively, we may write

$$\begin{cases} I_n(z) = I_n^+ \, e^{-jk_{zn}(z-z_n)} + I_n^- \, e^{+jk_{zn}(z-z_n)} \\ V_n(z) = \dfrac{I_n^+}{Y_n} e^{-jk_{zn}(z-z_n)} - \dfrac{I_n^-}{Y_n} e^{+jk_{zn}(z-z_n)} \end{cases} \quad (2)$$

where $Y_n = 1/Z_n$.

We refer to (1) and (2) as the voltage formulation and current formulation respectively. These equations are dual equations: letting $V \to I$, $I \to V$, and $Z \to Y$ in (1), we obtain (2).

By enforcing the continuity of voltage and current at the interface between TL sections n and $n+1$, we obtain the relationship

$$\begin{bmatrix} V_n^+ \\ V_n^- \end{bmatrix} = [\![T_n]\!] \begin{bmatrix} V_{n+1}^+ \\ V_{n+1}^- \end{bmatrix} \qquad (3)$$

where $[\![T_n]\!]$ is the transmission matrix (or T-matrix) of layer n, given as

$$[\![T_n]\!] = \frac{1}{2} \begin{bmatrix} \left(1 + \frac{Z_n}{Z_{n+1}}\right) e^{j\theta_n} & \left(1 - \frac{Z_n}{Z_{n+1}}\right) e^{j\theta_n} \\ \left(1 - \frac{Z_n}{Z_{n+1}}\right) e^{-j\theta_n} & \left(1 + \frac{Z_n}{Z_{n+1}}\right) e^{-j\theta_n} \end{bmatrix} \qquad (4)$$

where

$$\theta_n = k_{zn} d_n, \quad d_n = z_{n+1} - z_n .$$

We will use the voltage formulation (3)-(4) for TE waves ($\alpha = h$), and the dual current formulation for TM waves ($\alpha = e$). this way, both wave types can be handled using one form of T-matrix:

$$[\![T_n]\!] = \frac{1}{2} \begin{bmatrix} (1+Q_n)e^{j\theta_n} & (1-Q_n)e^{j\theta_n} \\ (1-Q_n)e^{-j\theta_n} & (1+Q_n)e^{-j\theta_n} \end{bmatrix} \qquad (5)$$

where $\qquad Q_n = q_n \dfrac{k_{z,n+1}}{k_{zn}}$

with

$$q_n = \begin{cases} \dfrac{\epsilon_{tn}}{\epsilon_{t,n+1}}, & \alpha = e \quad (TM) \\ \\ \dfrac{\mu_{tn}}{\mu_{t,n+1}}, & \alpha = h \quad (TE) \end{cases} \qquad (6)$$

Using (3), we may now relate the forward and backward wave amplitudes in layers 1 and N as

$$\begin{bmatrix} V_1^+ \\ V_1^- \end{bmatrix} = \underbrace{[\![T_1]\!][\![T_2]\!] \cdots [\![T_{N-1}]\!]}_{\equiv [\![T]\!]} \begin{bmatrix} V_N^+ \\ V_N^- \end{bmatrix} \qquad (7)$$

where

$$[T] = \begin{bmatrix} T_{11} & T_{12} \\ T_{21} & T_{22} \end{bmatrix} \qquad (8)$$

is the global T-matrix of multilayer.

We are interested in source-free solutions, which are the eigenmodes of the multilayer. If the structure is open below and above, we must have $V_1^+ = 0$ and $V_N^- = 0$, which leads to

$$\begin{bmatrix} 0 \\ V_1^- \end{bmatrix} = \begin{bmatrix} T_{11} & T_{12} \\ T_{21} & T_{22} \end{bmatrix} \begin{bmatrix} V_N^+ \\ 0 \end{bmatrix}$$

Non-trivial solutions of this system only exist if

$$f(k_\rho) \equiv T_{11} = 0 \qquad (9)$$

The roots (zeros) of the "dispersion function" $f(k_\rho)$ are the sought after "poles" in the open multilayer case.

Eq. (9) is applicable to both TE and TM wave types, provided that the appropriate form of q_n is selected in (6).

Note that the ~~roots~~ of (9) cannot depend on the location of the numerical interface z_1, which is best moved to z_2 (i.e. $\theta_1 = 0$) before $[T_1]$ is computed.

Consider next the effect of surface impedance planes at z_1 and z_{N+1} on the dispersion function.

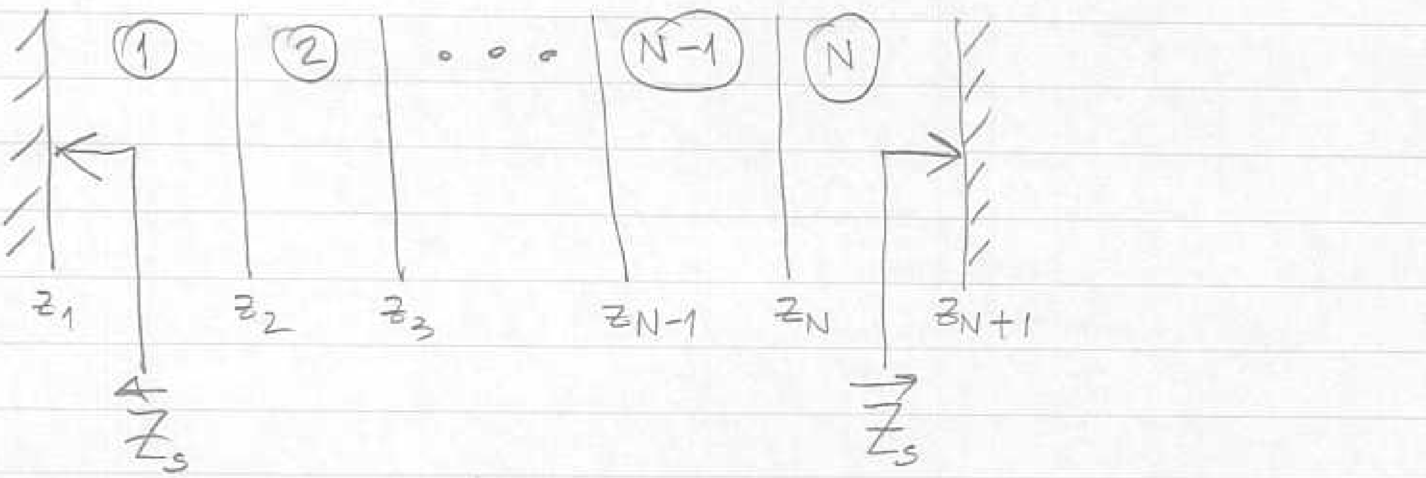

Let

$$\begin{bmatrix} V_1(z_1) \\ I_1(z_1) \end{bmatrix} \equiv \begin{bmatrix} V_1 \\ I_1 \end{bmatrix}, \quad \begin{bmatrix} V_N(z_{N+1}) \\ I_N(z_{N+1}) \end{bmatrix} \equiv \begin{bmatrix} V_{N+1} \\ I_{N+1} \end{bmatrix}$$

From (1) specialized to layer N, we find

$$\begin{bmatrix} V_{N+1} \\ I_{N+1} \end{bmatrix} = \begin{bmatrix} 1 & 1 \\ \frac{1}{Z_N} & -\frac{1}{Z_N} \end{bmatrix} \begin{bmatrix} e^{-j\theta_N} & 0 \\ 0 & e^{j\theta_N} \end{bmatrix} \begin{bmatrix} V_N^+ \\ V_N^- \end{bmatrix}$$

$$\equiv \begin{bmatrix} \vec{Z}_s \\ 1 \end{bmatrix} I_{N+1}$$

since $V_{N+1} = \vec{Z}_s I_{N+1}$.

Solving the above, we obtain

$$\begin{bmatrix} V_N^+ \\ I_N^+ \end{bmatrix} = \begin{bmatrix} (\vec{Z}_s + Z_N) e^{j\theta_N} \\ (\vec{Z}_s - Z_N) e^{-j\theta_N} \end{bmatrix} \frac{I_{N+1}}{2} \qquad (10)$$

In the 1st layer we have

$$\begin{bmatrix} V_1 \\ I_1 \end{bmatrix} = \begin{bmatrix} 1 & 1 \\ \frac{1}{Z_1} & -\frac{1}{Z_1} \end{bmatrix} \begin{bmatrix} V_1^+ \\ I_1^+ \end{bmatrix} \qquad (11)$$

and

$$V_1 = -\overset{\leftarrow}{Z}_s I_1$$

which we may write as

$$\left[1,\ \overleftarrow{Z}_s\right]\begin{bmatrix} V_1 \\ I_1 \end{bmatrix} = 0 \qquad (12)$$

Finally, using (7)-(8) and (10)-(12), we obtain the dispersion relation

$$f(k_\rho) = \left[\left(1+\frac{\overleftarrow{Z}_s}{Z_1}\right),\left(1-\frac{\overleftarrow{Z}_s}{Z_1}\right)\right] \times \begin{bmatrix} T_{11} & T_{12} \\ T_{21} & T_{22} \end{bmatrix}\begin{bmatrix} (\overrightarrow{Z}_s+Z_N)\,e^{j\theta_N} \\ (\overrightarrow{Z}_s-Z_N)\,e^{-j\theta_N} \end{bmatrix} = 0 \qquad (13)$$

Repeating the above steps with the current formulation, we derive the alternative expression:

$$f(k_\rho) = \left[\left(\overleftarrow{Z}_s+Z_1\right),\left(\overleftarrow{Z}_s-Z_1\right)\right] \times \begin{bmatrix} T_{11} & T_{12} \\ T_{21} & T_{22} \end{bmatrix}\begin{bmatrix} \left(1+\frac{\overrightarrow{Z}_s}{Z_N}\right)e^{j\theta_N} \\ \left(1-\frac{\overrightarrow{Z}_s}{Z_N}\right)e^{-j\theta_N} \end{bmatrix} = 0 \qquad (14)$$

Recall that the voltage formulation is used in TE ($\alpha = h$) case and the current formulation in TM ($\alpha = e$) case.

Both (13) and (14) can be specialized to PEC and PMC shielding by letting the appropriate Z_s approach 0 or ∞, respectively.

In the case of a single layer sandwiched between two impedance planes, (13) and (14) are applicable with N=1 and the T-matrix replaced by unit matrix.

Dispersion relations (13) and (14) can be written as

$$f(k_\rho) = [a_+, a_-] \, [\![T]\!] \begin{bmatrix} b_+ \, e^{j\theta_N} \\ b_- \, e^{-j\theta_N} \end{bmatrix} \qquad (15)$$

where

$$a_\pm^h = 1 \pm A_1^h k_{z1}^h$$

$$b_\pm^h = A_N^h \pm \frac{1}{k_{zN}^{(h)}}$$

$$a_{\pm}^{e} = A_1^{e} \pm k_{z1}^{e}$$

$$b_{\pm}^{e} = 1 \pm \frac{A_N^{e}}{k_{zN}^{c}}$$

with

$$A_1^{\alpha} = \begin{cases} \epsilon_{t1} \overleftarrow{Z}_s , & \alpha = e \quad (TM) \\ \dfrac{\overleftarrow{Z}_s}{\mu_{t1}} , & \alpha = h \quad (TE) \end{cases}$$

$$A_N^{\alpha} = \begin{cases} \epsilon_{tN} \overrightarrow{Z}_s , & \alpha = e \quad (TM) \\ \dfrac{\overrightarrow{Z}_s}{\mu_{tN}} , & \alpha = h \quad (TE) \end{cases}$$

It is understood that surface impedances Z_s are normalized to the intrinsic impedance of free space, η_0:

$$\frac{\overleftrightarrow{Z}_s}{\eta_0} \longrightarrow \overleftrightarrow{Z}_s$$

$$\eta_0 = \sqrt{\frac{\mu_0}{\epsilon_0}}$$

The procedure that will be employed to find the roots of the dispersion relations (9) or (15) requires the computation of the derivatives of the dispersion function.

In the general case (15), we obtain

$$f'(k_\rho) = [a_+, a_-]' [\![T]\!] \begin{bmatrix} b_+ e^{j\theta_N} \\ b_- e^{-j\theta_N} \end{bmatrix} + [a_+, a_-] [\![T]\!]' \begin{bmatrix} b_+ e^{j\theta_N} \\ b_- e^{-j\theta_N} \end{bmatrix} + [a_+, a_-] [\![T]\!] \begin{bmatrix} b_+ e^{j\theta_N} \\ b_- e^{-j\theta_N} \end{bmatrix}' \qquad (16)$$

where primes denote differentiation. Note that in the single layer case the second term in (16) is zero.

All functions in (16) depend on k_ρ via k_ρ^2, hence it is convenient to use the chain rule:

$$\frac{\partial}{\partial k_\rho} = (2k_\rho) \frac{\partial}{\partial (k_\rho^2)}$$

and differentiate w.r.t. k_ρ^2

Here are some of the details:

$$\frac{\partial}{\partial(k_\rho^2)} k_{zn} = -\frac{1}{2\nu_n k_{zn}}$$

$$\frac{\partial}{\partial(k_\rho^2)} \frac{1}{k_{zn}} = \frac{1}{2\nu_n k_{zn}^3}$$

$$\frac{\partial}{\partial(k_\rho^2)} e^{\pm j\theta_N} = \mp \frac{j\theta_N}{2\nu_N k_{zN}^2} e^{\pm j\theta_N}$$

$$\frac{\partial}{\partial(k_\rho^2)} \left[\left(A_N \pm \frac{1}{k_{zN}}\right) e^{\pm j\theta_N}\right] = \pm \frac{e^{\pm j\theta_N}}{2\nu_N k_{zN}^3}$$

$$\times \left[1 - j\theta_N (A_N k_{zN} \pm 1)\right]$$

$$\frac{\partial}{\partial(k_\rho^2)} \left[\left(1 \pm \frac{A_N}{k_{zN}}\right) e^{\pm j\theta_N}\right] = \pm \frac{e^{\pm j\theta_N}}{2\nu_N k_{zN}^3}$$

$$\times \left[A_N - j\theta_N (k_{zN} \pm A_N)\right]$$

$$\frac{\partial}{\partial(k_\rho^2)}\left(1 \pm A_1 k_{z1}\right) = \mp \frac{A_1}{2\,\nu_1 k_{z1}}$$

$$\frac{\partial}{\partial(k_\rho^2)}\left(A_1 \pm k_{z1}\right) = \mp \frac{1}{2\,\nu_1 k_{z1}}$$

$$\frac{\partial}{\partial(k_\rho^2)} \frac{k_{z,n+1}}{k_{zn}} = - \frac{1}{2\,\nu_{n+1} k_{z,n+1} k_{zn}}$$

$$\times \left[1 - \frac{\nu_{n+1}}{\nu_n}\left(\frac{k_{z,n+1}}{k_{zn}}\right)^2 \right]$$

$$\left(1 \pm \frac{Z_n}{Z_{n+1}}\right) e^{\pm j\theta_n} = \pm \frac{q_n k_{z,n+1}}{k_{zn}}$$

$$\times \left(1 \pm \frac{k_{zn}}{q_n k_{z,n+1}}\right) e^{\pm j\theta_n}$$

these signs
are related

$$\frac{\partial}{\partial(k_\rho^2)}\left[\left(1 \pm \frac{q_n k_{z,n+1}}{k_{zn}}\right) e^{\pm j\theta_n}\right] = \pm \frac{1}{2\,\nu_n\, k_{zn}^2}$$

$$\times \frac{q_n k_{z,n+1}}{k_{zn}} \left\{ \left[1 - \frac{\nu_n}{\nu_{n+1}} \left(\frac{k_{zn}}{k_{z,n+1}}\right)^2 \right] \right.$$

$$\left. \mp j\theta_n \left(1 \pm \frac{k_{zn}}{q_n k_{z,n+1}}\right) \right\} e^{\pm j\theta_n}$$

these signs are related

Using these formulas, we may compute the local T-matrix $[\![T_n]\!]$, its derivative $[\![T_n]\!]'$, the "end functions"

$$[a_+, a_-], \quad \begin{bmatrix} b_+ \, e^{j\theta_N} \\ b_- \, e^{-j\theta_N} \end{bmatrix},$$

as well as their derivatives.

We still need an algorithm for computing the derivative of global T-matrix:

$$[\![T]\!]' = \left([\![T_1]\!] [\![T_2]\!] \cdots [\![T_{N-1}]\!] \right)'$$

We use a recursive procedure that accumulates the global T-matrix $[\![T]\!]$ and its derivative $[\![T]\!]'$ as the layer index n is incremented from 1 to $N-1$.

At the n-th step, we have

$$[\![T]\!]_n = \prod_{i=1}^{n} [\![T_i]\!] = [\![T]\!]_{n-1} [\![T_n]\!] ,$$

$$[\![T]\!]'_n = [\![T]\!]'_{n-1} [\![T_n]\!] + [\![T]\!]_{n-1} [\![T_n]\!]' ,$$

which suggests the following flow of computations:

$$[\![T]\!] = [\![T_1]\!] \; ; \; [\![T]\!]' = [\![T_1]\!]'$$

do $n = 2, N-1$

$$[\![T]\!]' = [\![T]\!]' [\![T_n]\!] + [\![T]\!] [\![T_n]\!]'$$

$$[\![T]\!] = [\![T]\!] [\![T_n]\!]$$

end do

Note that at each step we only compute the layer matrix $[\![T_n]\!]$ and its derivative.

An understanding of the analytical properties of the dispersion function is crucial for the success of the pole finder procedure.

Since k_{zn} is double-valued in the complex k_ρ-plane, it would appear from (5) and (7) that the global T-matrix has branch points at $\pm k^\alpha_{eff,n}$, $n = 1, 2, \ldots, N$, and is singular at $\pm k^\alpha_{eff,n}$, $n = 1, 2, \ldots, N-1$.

To investigate this, consider the product

$$[M] \equiv [T_{n-1}][T_n] = \begin{bmatrix} M_{11} & M_{12} \\ M_{21} & M_{22} \end{bmatrix}$$

From (5) we find (omitting the 1/4 factor)

$$M_{11} = (1+Q_{n-1})(1+Q_n)\, e^{j(\theta_{n-1}+\theta_n)} + (1-Q_{n-1})(1-Q_n)\, e^{j(\theta_{n-1}-\theta_n)}$$

Note that if we let $k_{zn} \to -k_{zn}$, the signs of Q_{n-1}, Q_n, and θ_n will change, but the result remains unchanged.

Expanding the expression for M_{11}, we further find

$$M_{11} = (1 + Q_{n-1} + Q_n + Q_{n-1} Q_n)\, e^{j(\theta_{n-1} + \theta_n)}$$
$$+ (1 - Q_{n-1} - Q_n + Q_{n-1} Q_n)\, e^{j(\theta_{n-1} - \theta_n)}$$

As $k_\rho \to k_{1eff,n}$, $k_{zn} \to 0$, $\theta_n \to 0$, and

$$M_{11} \to 2\,(1 + Q_{n-1} Q_n)\, e^{j\theta_{n-1}}$$
$$= 2\left(1 + q_{n-1} \frac{\cancel{k_{z,n}}}{k_{z,n-1}}\, q_n \frac{k_{z,n+1}}{\cancel{k_{zn}}}\right) e^{j\theta_{n-1}}$$

Note that M_{11} is finite at $k_{1eff,n}$.

Similar conclusions apply to the other elements of [M]. Hence, $k_{eff,n}$ is not a branch point of [M]; also, [M] is has a finite limit at this point. Evidently, [M] does not have poles either.

We therefore conclude that the global T-matrix of a multilayer is free of poles, has two pairs of branch points at $\pm k_{eff,1}$ and $k_{eff,N}$, and has an inverse-square root singularity at $\pm k_{eff,1}$.

For an unshielded multilayer, the dispersion function will have the same properties.

Consider next the effect of shielding in (15). In TM case, we find (omitting the ½ factor and the superscripts)

$$[a_+, a_-]\,[\![T_1]\!] = \Big[(A_1 + k_{z1})(1+Q_1)e^{j\theta_1} + (A_1 - k_{z1})(1-Q_1)e^{-j\theta_1},\ (A_1+k_{z1})(1-Q_1)e^{j\theta_1} + (A_1 - k_{z1})(1+Q_1)e^{-j\theta_1}\Big]$$

Clearly, the result is insensitive to the change of sign of k_{z1}, and there is no singularity at $k_\rho = \pm k_{eff,1}$. Hence, bottom shielding removes the branch points at $\pm k_{eff,1}$ and renders the dispersion function regular at these points.

Similarly, we find

$$[\![T_{N-1}]\!]\begin{bmatrix} b_+\, e^{j\theta_N} \\ b_-\, e^{-j\theta_N} \end{bmatrix} =$$

$$= \begin{bmatrix} (1+Q_{N-1})\left(1+\frac{A_N}{k_{zN}}\right)e^{j(\theta_{N-1}+\theta_N)} + (1-Q_{N-1})\left(1-\frac{A_N}{k_{zN}}\right)e^{j(\theta_{N-1}-\theta_N)} \\ (1-Q_{N-1})\left(1+\frac{A_N}{k_{zN}}\right)e^{-j(\theta_{N-1}-\theta_N)} + (1+Q_{N-1})\left(1-\frac{A_N}{k_{zN}}\right)e^{-j(\theta_{N-1}+\theta_N)} \end{bmatrix}$$

Recalling that $Q_{N-1} = q_{N-1}\dfrac{k_{zN}}{k_{z,N-1}}$, we see that the above result is unaffected by the change of the sign of k_{zN}, and is regular as $k_\rho \to \pm k_{eff,N}$ and $k_{zN} \to 0$.

Therefore, top shielding removes the branch points at $\pm k_{eff,N}$. Also, the dispersion function remains bounded at these points.

As a word of caution, one must avoid the temptation to modify the dispersion function by multiplying or dividing it by some factor (other than a constant), which does not affect the roots, but may destroy the nice analytical properties of $f(k_p)$.

For example, the presence of growing exponentials in (5) is clearly a disadvantage, and one might be tempted to factor out $e^{i\theta_n}$ from $[\![T_n]\!]$ in order to reduce the danger of overflows. However, such a device would introduce branch points at $k_{\mathrm{eff},n}$ and render the pole search procedure that we describe next no longer applicable.

The problem before us is to find all roots of

$$f(z) = 0$$

enclosed by a specified closed contour C in the complex z-plane. We assume that $f(z)$ is an entire function inside and on C and that it does not have any zeros on C.

In our case, of course f is the dispersion function of the multilayer. Although we are ultimately interested in the roots in the k_0-plane, it will be advantageous to first map f to another plane, called the z-plane which in certain situations facilitates the root search.

Consider the integrals

$$s_k = \frac{1}{2\pi j} \oint_C z^k \frac{f'(z)}{f(z)} dz, \qquad (17)$$

$k = 0, 1, \ldots$

where C is traversed in the positive sense (i.e., counter-clockwise).

We will refer to the integrals s_k as Newton moments.

Let z_i, $i=1,\dots,N$ be the zeros of $f(z)$ inside C. (Note that N has nothing to do with the number of layers, for which the same symbol was used.)

It follows from the residue theorem that

$$s_0 = N \tag{18}$$

and

$$\left\{\begin{array}{l} s_1 = z_1 + z_2 + \cdots + z_N \\ s_2 = z_1^2 + z_2^2 + \cdots + z_N^2 \\ \vdots \\ s_N = z_1^N + z_2^N + \cdots + z_N^N \end{array}\right. \tag{19}$$

The $N \times N$ system of nonlinear equations (19) can in principle be solved for the N roots $\{z_1, \dots, z_N\}$. ~~This~~ This, of course, is a rather daunting task.

Delves & Lyness have shown that the zeros $\{z_1, \cdots, z_N\}$ can be found as roots of a polynomial

$$z^N + \sigma_1 z^{N-1} + \cdots + \sigma_N = 0 \qquad (20)$$

where the coefficients are related to the Newton moments s_k by the Newton identities:

$$\begin{cases} s_1 + \sigma_1 = 0 \\ s_2 + s_1\sigma_1 + 2\sigma_2 = 0 \\ \vdots \\ s_N + s_{N-1}\sigma_1 + s_{N-2}\sigma_2 + \cdots + s_1\sigma_{N-1} + N\sigma_N = 0 \end{cases} \qquad (21)$$

The triangular system (21) can be solved by forward substitutions in $N(N-1)/2$ operations.

The roots of the polynomial (20) are readily found by Laguerre's method.

These roots can be further refined by Newton-Raphson method, since the derivative of $f(z)$ is available.

Unfortunately the map from Newton moments $\{s_1, \ldots, s_N\}$ to the coefficients $\{\sigma_1, \ldots, \sigma_N\}$ is usually ill-conditioned. Also, the polynomial roots are extremely sensitive to perturbations of the coefficients.

As a result, in practical implementations of Delves-Lyness algorithm the maximum number of zeros in C is usually limited to 4–5. Our experiments have shown that this number may be doubled in many cases. However even if the limit on N is pushed to 8-10, this number is often exceeded in the case of multilayered media at higher frequencies, and the subdivision of the search region C into smaller regions is required.

The search region subdivision increases the likelyhood that the region boundary passes near a zero of $f(z)$, which may cause the contour integrals s_k to diverge.

In such a case, the contour C must be shifted in small increments, until convergent integrals are obtained.

The contour shifting introduces a possibility that some zeros may end up being included in two or more adjacent subregions. Such duplicates, if found, must be eliminated at the post-processing stage.

The above enhancements have been successfully implemented here.

We have opted for rectangular search regions with edges parallel to the coordinate axes — see the illustration below, where an example search "box" is erected in k_ρ-plane. The box is defined by its lower-left and upper-right vertices (x_1, y_1) and (x_2, y_2).

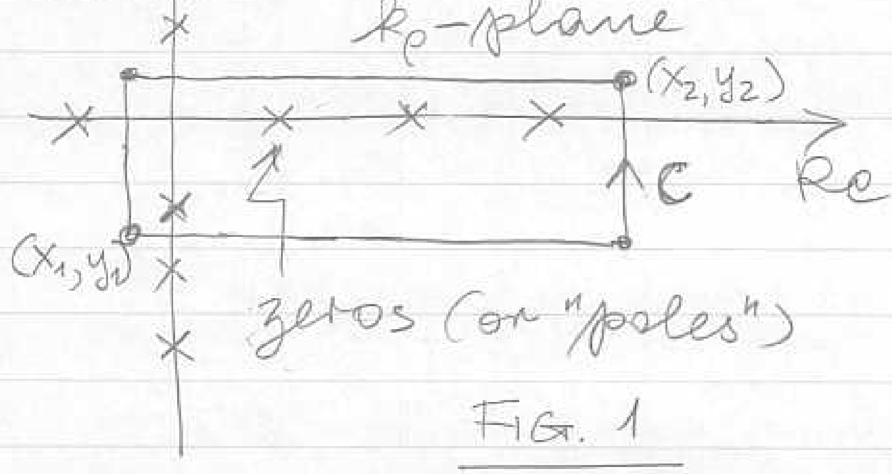

FIG. 1

The zeros marked in Fig. 1 are also poles of the Green function of the layered medium, and we will use both terms, hopefully without causing confusion.

Poles are the only singularities in Fig. 1, hence this picture may correspond to a layered medium shielded on both sides. (This medium is lossless, because the poles are distributed on the real and imaginary axes.) It is well known that the real-axis poles must fall to the left of $k_{eff,max}$ – the maximum effective wavenumber of the multilayer. (Some of the real-axis poles, and all of the imaginary axis's poles are the propagation constants of the parallel-plate waveguide formed by the shield planes.)

The objective here is not to find "all" poles, but only the "significant" poles, i.e. those close to the positive real axis.

If the multilayer is unshielded (open) below or above, a branch point will appear in the 4-th quadrant of k_ρ-plane necessitating the introduction of a branch cut, as illustrated below.

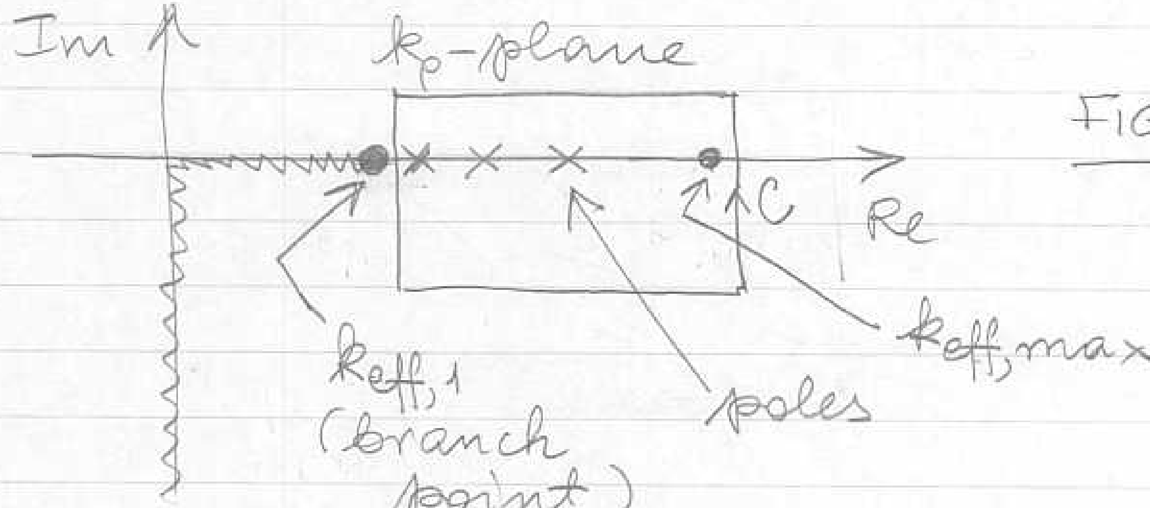

FIG. 2

Observe that the search box cannot cross the branch cut, which may force it to pass arbitrarily close to the branch point, if all significant poles are to be enclosed. This will cause the integrals in (17) to diverge.

In fact, as we have seen, if the structure is open below, the dispersion function f will behave as

$$f \sim \frac{1}{k_{z1}}$$

and its derivative (here $z = k_\rho$)

$$f' \sim \frac{k_\rho}{\nu_1 k_{z1}^3}$$

for $k_\rho \to k_{eff,1}$. Hence, the logarithmic derivative of f in (17) behaves as

$$\frac{f'}{f} \sim \frac{k_\rho}{\nu_1 k_{z1}^2} \qquad (22)$$

which has a pole-like singularity.

Clearly, it is desirable to remove the $k_\rho = k_{eff,1}$ branch point by a suitable mapping from the k_ρ-plane to a new, z-plane.

The mapping that we use is given as

$$k_{z1} = k_1 \cos(z) \qquad (23)$$

which makes k_{z1} single-valued. (The plus sign is chosen to make the point $k_\rho = 0$ correspond to $z = 0$.)

From (23), we find

$$k_\rho = k_{eff,1} \sin(z) \qquad (24)$$

and the Jacobian

$$\frac{\partial k_\rho}{\partial z} = k_{eff,1} \cos(z) \qquad (25)$$

Inverting (24), we obtain

$$z = \frac{1}{j} \ln\left(\frac{j\frac{k_\rho}{\mu_1} + k_{z1}}{k_1} \right) \pm 2n\pi \qquad (26)$$

Note that when $k_{z1} = 0$ in (23) $z = \pi/2$, hence the branch point $k_{eff,1}$ in k_ρ-plane maps into the point $z = \pi/2 + j0$ (even if k_1 is complex-valued). Furthermore, using (22)-(25), we find that

$$\frac{f'}{f} \frac{\partial k_\rho}{\partial z} \longrightarrow \frac{\sin(z)}{\cos(z)} \qquad (27)$$

as $z \to \pi/2$. Hence, the $k_{eff,1}$ branch point contributes a spurious pole in the z-plane. We thus subtract the pole term (27) in (17), as follows:

$$S_k = \frac{1}{2\pi j} \oint_C z^k \left[\frac{f'(z)}{f(z)} - \frac{\sin(z)}{\cos(z)} \right] dz \qquad (28)$$

The k_ρ-plane of Fig. 2 is part of a 2-sheeted Riemann surface.

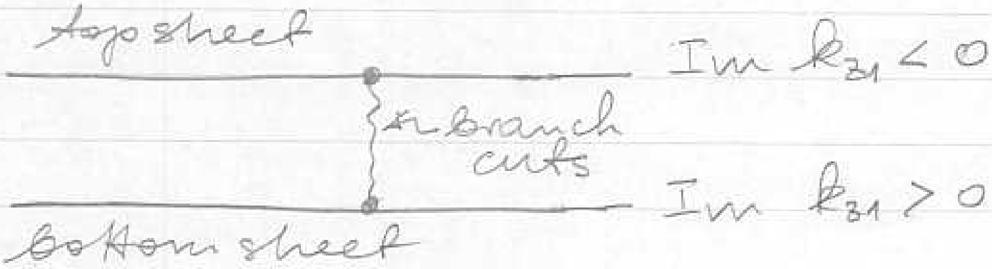

FIG. 3

Under the mapping (26) the branch cuts are "opened up" and the two Riemann sheets are put side-by-side in a vertical strip of width 2π.

The map of the 1st and fourth quadrants is illustrated in the figure below for lossless and lossy cases.

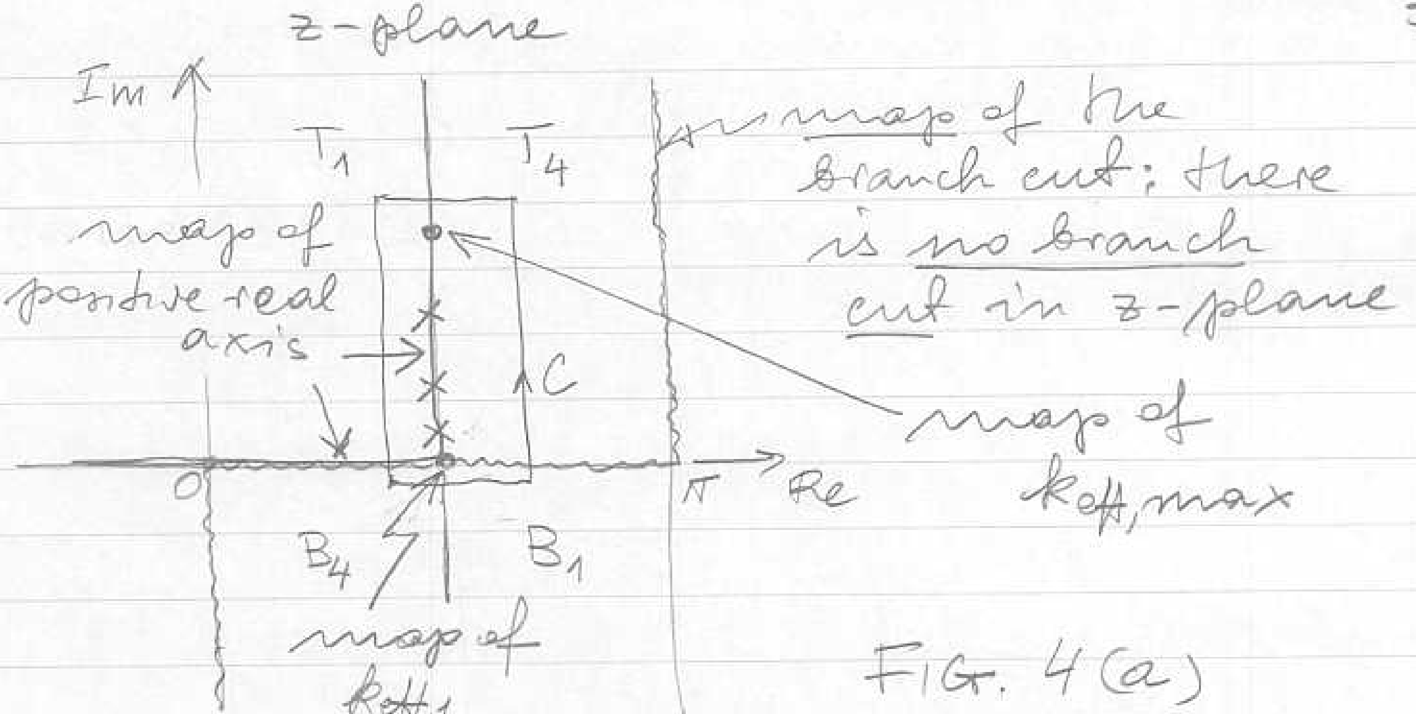

FIG. 4 (a)

The symbols T_1 and T_4 indicate the maps of the 1st and fourth quadrants of the top sheet of the Riemann surface. Similarly, the symbols B_1 and B_4 denote the maps of the 1st and fourth quadrants of the bottom sheet of the Riemann surface.

Note that the rectangular search box is "anchored" by $\pi/2$ (the map of $k_{eff,1}$) and the map of $k_{eff,max}$.

The pole at $z = \pi/2$ has been subtracted, but the contour C is shifted slightly down, in order not to "step" on the subtracted singularity.

When $k_{eff,1}$ is complex-valued the map of Fig. 4(a) is distorted, as shown below.

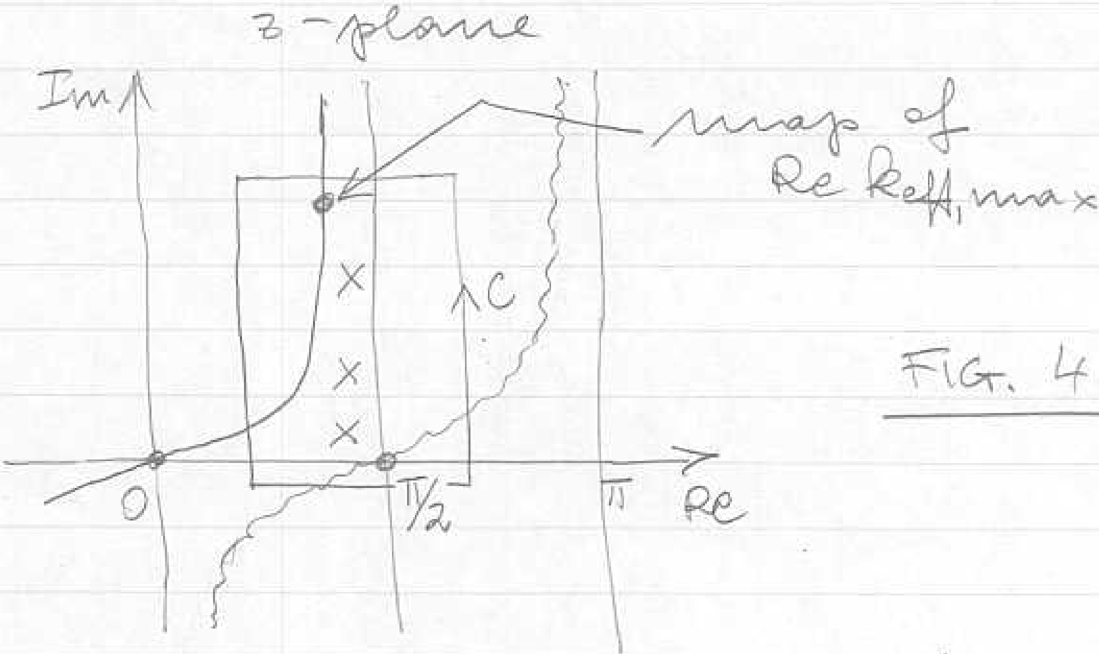

FIG. 4(b)

The search box selection is more difficult in this case, although $\pi/2$ and the map of $k_{eff,max}$ may still be used as anchors. There is a possibility of missing some significant poles if the box is too small. At the same time, some unwanted bottom-sheet poles may be enclosed – quite a few of them, if the box is too large.

If the structure is open above and shielded below, a mapping described above is also employed except that $k_{eff,1}$ is replaced by $k_{eff,N}$. In this case the singularity at $\pi/2$ does not arise and there is no need to subtract the pole term as in (28).

If the structure is open below and above and the half-space media are identical, we still use the map (24).

If the half-space media are different, there are two pairs of branch points at $\pm k_{eff,1}$ and $\pm k_{eff,N}$, and the Riemann surface has four leafs, as illustrated below.

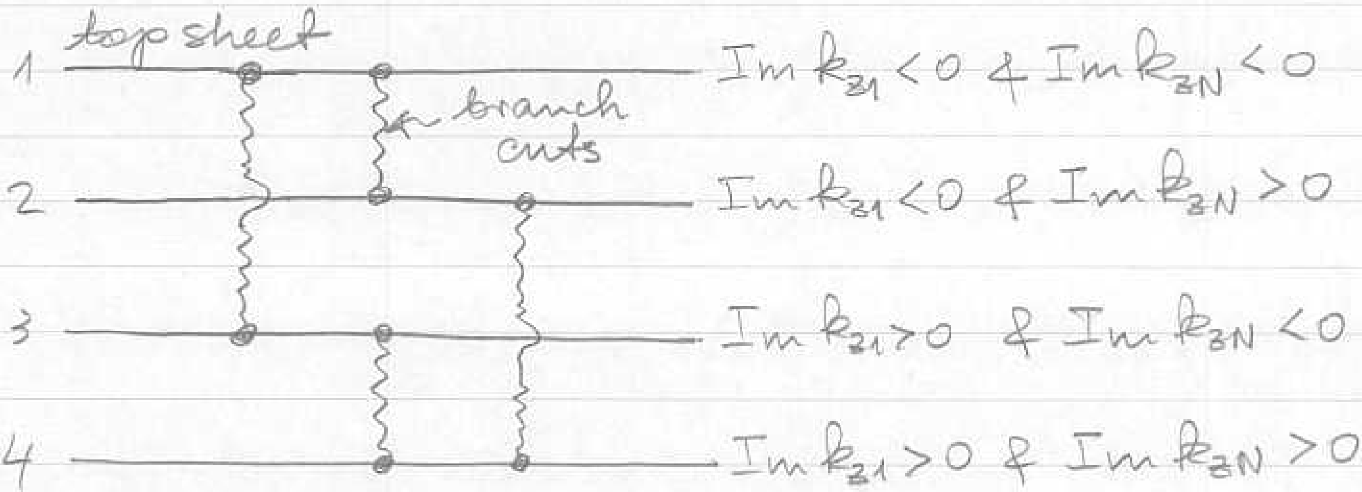

FIG. 5

the fourth quadrant of the k_ρ-plane now has two branch cuts, as shown below.

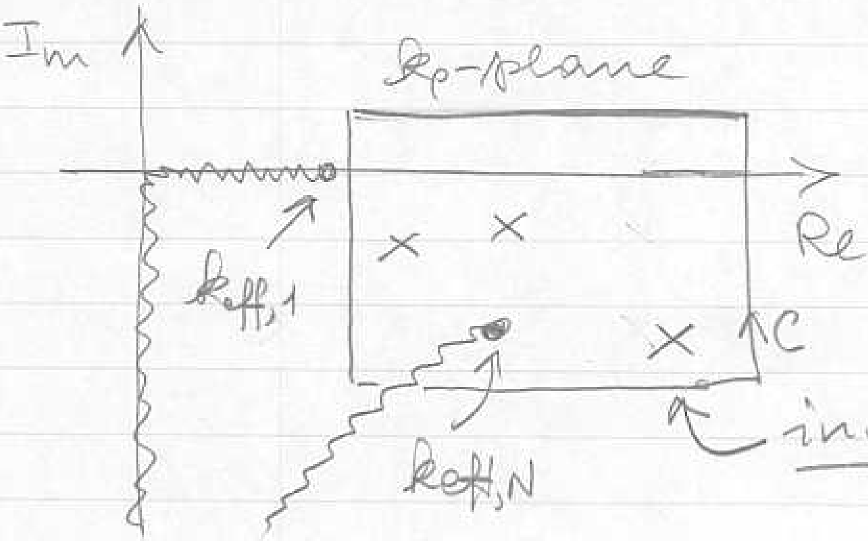

FIG. 6

It may now be impossible to select a search box that captures all significant poles and does not cross a branch cut.

Hence, the best strategy is to map the k_ρ-plane into a z-plane in such a way, that both branch point pairs are removed.

We employ the following mapping in this case (open top and bottom different half-space media):

$$\begin{cases} k_{z1} = \frac{1}{\lambda_1}\left(e^{jz} + R\, e^{-jz}\right) \\ k_{zN} = \frac{1}{\lambda_N}\left(e^{jz} - R\, e^{-jz}\right) \end{cases} \qquad (29)$$

where the coefficient R is given as

$$R = \frac{1}{4}\left(k_{eff,1}^2 - k_{eff,N}^2\right) \qquad (30)$$

From the above we find that

$$k_\rho^2 = S - \left(e^{j2z} + R^2 e^{-j2z}\right) \qquad (31)$$

where

$$S = \frac{1}{2}\left(k_{eff,1}^2 + k_{eff,N}^2\right) \qquad (32)$$

The Jacobian follows from (31):

$$\frac{\partial k_\rho^2}{\partial z} = -2j\left(e^{jz} + R\, e^{-jz}\right)\left(e^{jz} - R\, e^{-jz}\right) \qquad (33)$$

Inverting (31), we find

$$z = \frac{1}{j} \log \left(\frac{\lambda_1 k_{z1} + \lambda_N k_{zN}}{2} \right) \pm 2n\pi \qquad (34)$$

Let us investigate the maps of the branch points $k_\rho = \pm k_{eff,1}$ and $\pm k_{eff,N}$.

As $k_\rho \to \pm k_{eff,1}$, $k_{z1} \to 0$, and

$$z \to z_1 = \frac{1}{2j} \log(-R) \qquad (35)$$

As $k_\rho \to \pm k_{eff,N}$, $k_{zN} \to 0$, and

$$z \to z_2 = \frac{1}{2j} \log R \qquad (36)$$

Assume, for simplicity, real-valued $k_{eff,1}$ and $k_{eff,N}$ (i.e., the bottom and top half-spaces are lossless)

<u>Case 1</u>: $k_{eff,1} < k_{eff,N} \Rightarrow R = -|R|$

$$z_1 = 0 - j \log \sqrt{|R|}$$

$$z_2 = \pm \frac{\pi}{2} - j \log \sqrt{|R|}$$

<u>Case 2</u>: $k_{eff,1} > k_{eff,N} \Rightarrow R = |R|$

$$z_1 = \pm\frac{\pi}{2} - j\log\sqrt{|R|}$$

$$z_2 = 0 - j\log\sqrt{|R|}$$

For complex-valued $k_{eff,1}$ and $k_{eff,N}$, R is complex and the general expressions (35) and (36) must be used.

The $k_\rho = 0$ point maps as

$$z_0 = -j\log\left(\frac{k_{eff,1} + k_{eff,N}}{2}\right) \qquad (37)$$

For lossless exterior media, this is a point on negative-imaginary axis.

As with the mapping (26), the $k_{eff,1}$ branch point contributes a spurious pole in the z-plane when (34) is employed.

It can be shown that, as $z \to z_1$,

$$\frac{f'}{f}\frac{\partial k_p}{\partial z} \to \frac{1}{j}\,\frac{e^{jz} - R e^{-jz}}{e^{jz} + R e^{-jz}}$$

We subtract this term when the Newton moments are computed:

$$S_k = \frac{1}{2\pi j}\oint_C z^k \left[\frac{f'(z)}{f(z)} - \frac{1}{j}\,\frac{e^{jz} - R e^{-jz}}{e^{jz} + R e^{-jz}}\right] dz \quad (38)$$

Some typical z-plane maps of the 1st and fourth quadrants of the ~~top~~ sheet of the k_p Riemann surface are shown below.

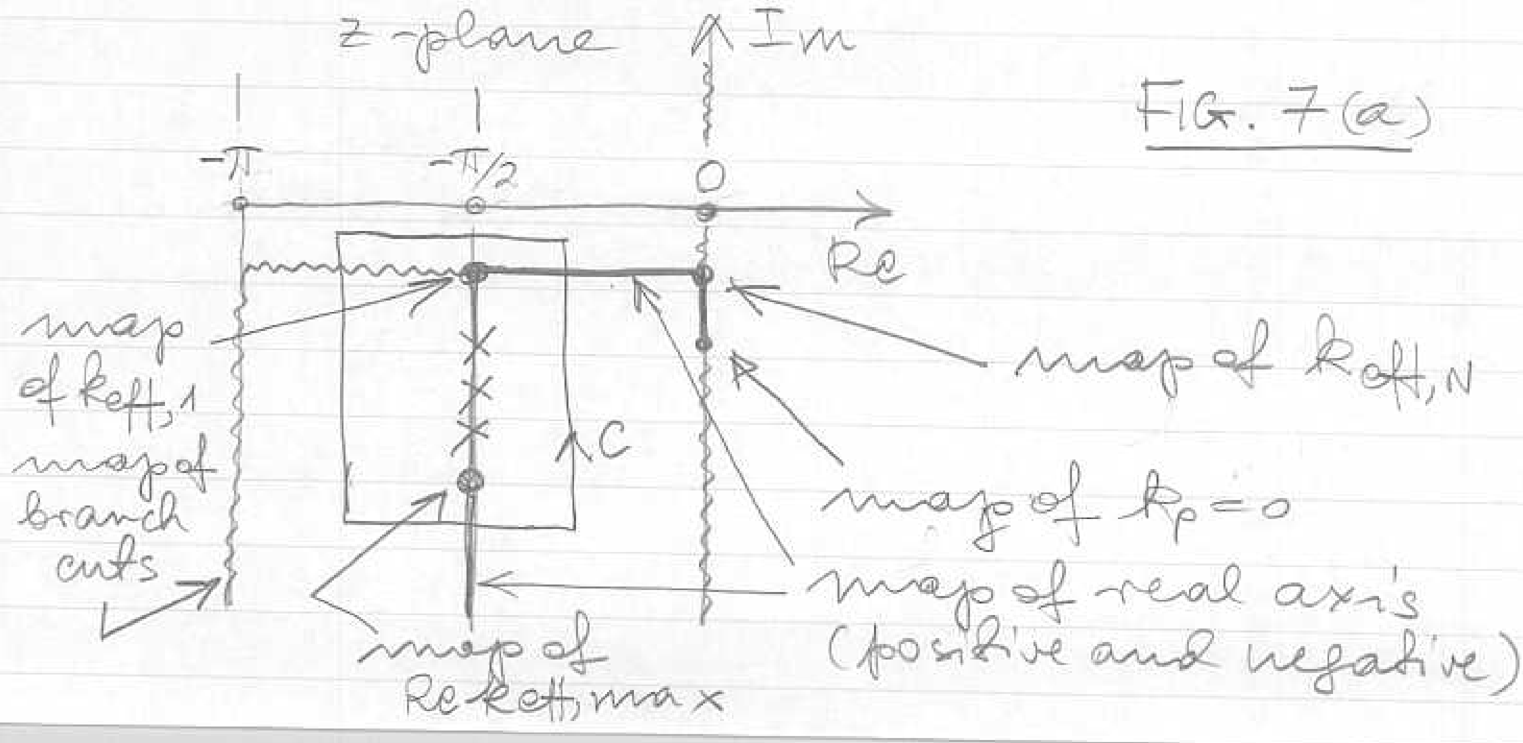

FIG. 7(a)

the above picture pertains to real-valued $k_{eff,1}$ and $k_{eff,N}$ (lossless exterior media). If $k_{eff,1}$ and $k_{eff,N}$ are complex-valued, a more complicated picture obtains, as illustrated below.

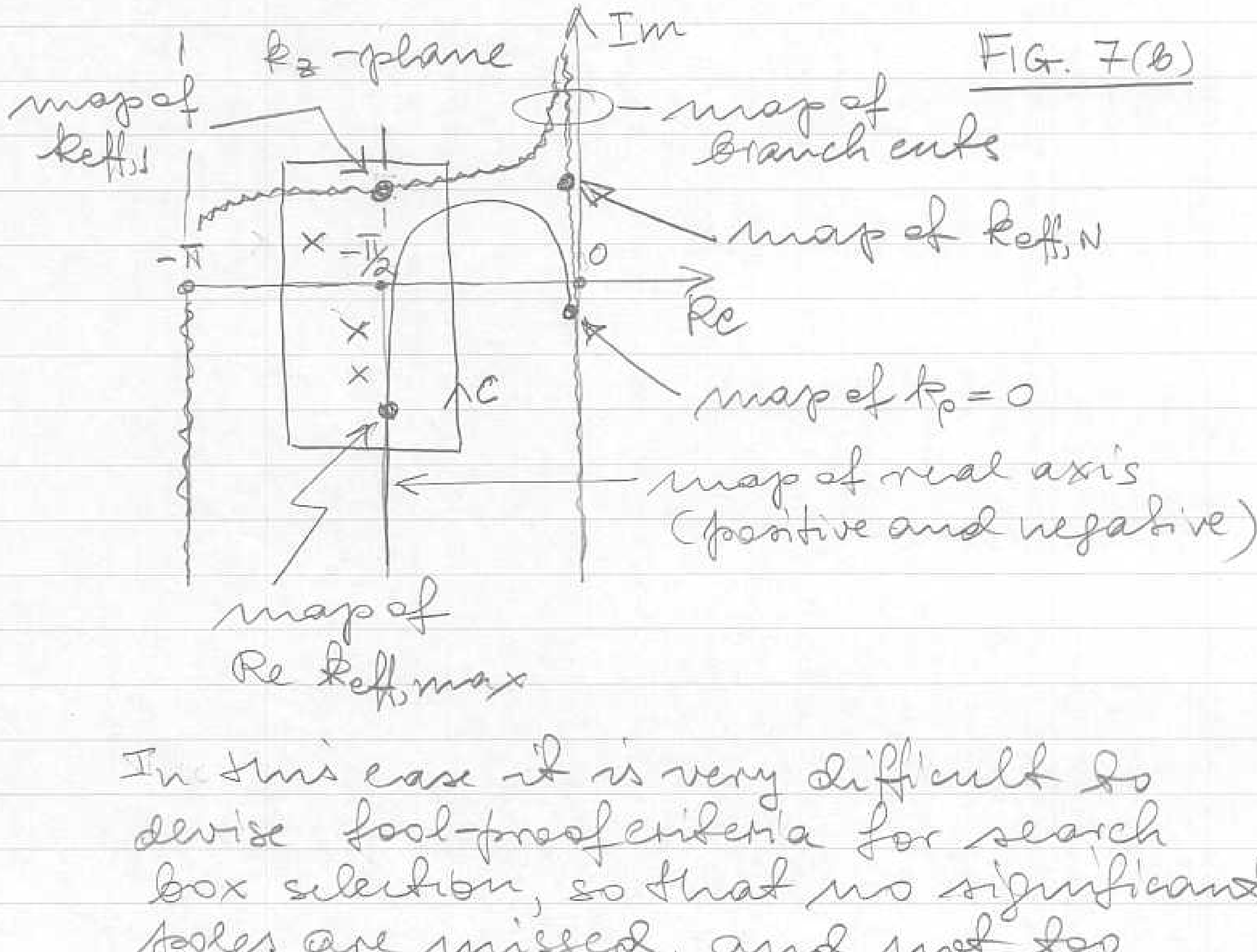

FIG. 7(b)

In this case it is very difficult to devise fool-proof criteria for search box selection, so that no significant poles are missed, and not too many improper poles are enclosed.

We use the maps of $k_{eff,1}$, $k_{eff,N}$ and $k_{eff,max}$ as anchor points.

When k_ρ-plane mapping is used, the poles are located in the z-plane and must be mapped back using (24) or (31).

However, some of the poles found may be improper and not of interest in the present context. Hence, a test is required to weed out the unwanted poles.

To determine if a pole z_i lies on the top sheet, we erect a small circular contour C_i centered at z_i with a radius r selected so that C_i does not enclose any other poles or branch points, and evaluate the integral

$$S_0 = \frac{1}{2\pi} \int_0^{2\pi} \left. \frac{f'(z)}{f(z)} \right|_{z = z_i + re^{j\varphi}} re^{j\varphi} \, d\varphi \qquad (39)$$

In view of (17), s_0 should be 1 if the pole is on the top sheet, or zero if it belongs to one of the improper sheets.

The integral in (39) is evaluated by adaptive trapezoidal rule, which is most appropriate for periodic integrands. The tolerance can be quite loose, because we only need to determine if the result is close to 1 or to zero.

In contrast, the computation of the Newton moments (17) (also (28) and (38)) should be done with high precision. Since rectangular search boxes are employed, we apply on each of the four edges an adaptive quadrature based on Patterson's rules.

To make the computations efficient all the moments are integrated simultaneously, so that the logarithmic derivative of the dispersion function of the multilayer is only computed once at each point.

Furthermore, to prevent loss of accuracy when higher moments are computed, we shift each search box so that its origin coincides with the coordinate origin.

Hence, if the rectangle vertices are $z_1, \dots, z_4$, we compute the center point $z_{AVG} = \left(\sum_{i=1}^{4} z_i\right)/4$ and subtract it from z_i, $i = 1, \dots, 4$, to obtain a shifted box centered at the origin. The Newton moments are now computed as

$$S_k = \frac{1}{2\pi j} \oint_{C_{shifted}} z^k \left. \frac{f'(z)}{f(z)} \right|_{z = z + z_{AVG}} dz \qquad (40)$$

After the poles are located based on these modified moments, they must be shifted as

$$z_{pole} \rightarrow z_{pole} + z_{avg} \qquad (41)$$

The general computational flow chart of the polefinder package is shown in Fig. 8.

The number of poles in box #1 is found by computing s_0 using (17), (28) or (38), depending on the mapping in use. Failure may occur if the contour integral diverges or it is not close to an integer, or the number of poles found is too large to proceed with pole location.

As mentioned earlier, failure due to a divergent integral may occur if an edge of the search box passes too close to a pole (a zero of $f_i(z)$). To minimize this possibility, we generate a sequence of small random shifts and repeat the integration on the shifted edges until convergence is achieved or the maximum allowed number of re-tries is reached.

As a result of this procedure, the original search box may be slightly expanded.

the pole locations in box #2 are obtained by first computing N Newton moments simultaneously, using (17), (28), or (38). A high-order adaptive quadrature is employed on the search box last successfully used in box #1. Hence, the divergence of the integrals should not occur, since we are guaranteed that the search box edges are not too close to any poles.

From the Newton moments, the polynomial coefficients are found using (21), and the poles are computed as roots of the polynomial (20). The Laguerre method with root polishing is used to find the roots.

The poles found are next refined using the Newton-Raphson method using the dispersion function $f(z)$ of the multilayer and its derivative. Should this polishing fail, the poles are discarded and the error flag is set to failure.

If the procedure fails to reliably locate the poles in the search box, the box is split into four sub-boxes, and search is performed on the smaller boxes, which may be divided further, if necessary.

Since the boxes may be slightly expanded during the searches, some poles may end up being captured by more than one search box. Hence, after a successful search, only non-duplicate poles are kept.

Finally, since a search box may extend into what were improper sheets in the original k_p-plane, some of the poles found may be improper. Hence, the poles are tested and those on the top sheet flagged.

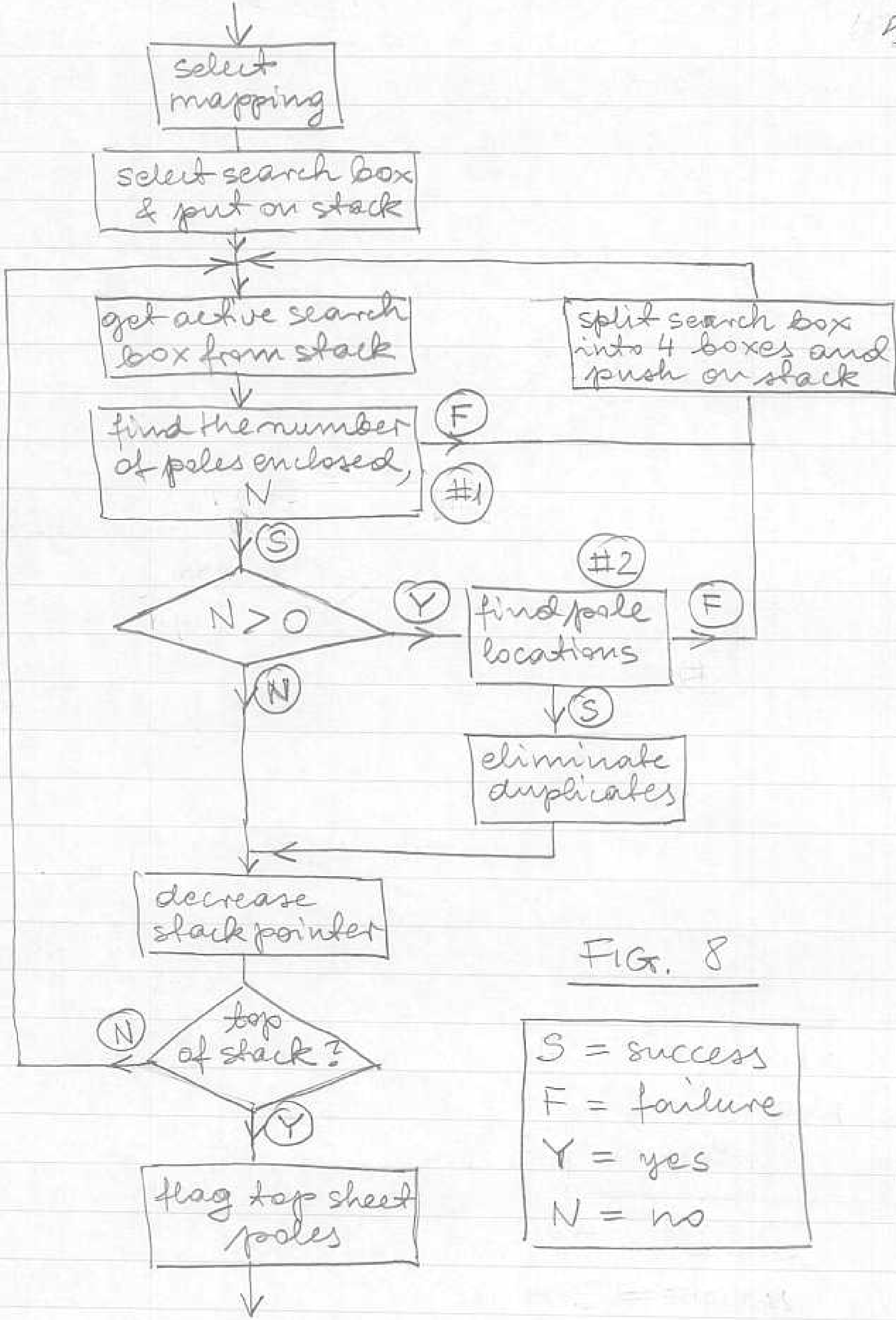

select mapping
select search box & put on stack
get active search box from stack
find the number of poles enclosed, N
F
#1
S
N > 0
Y
N
#2
find pole locations
F
S
eliminate duplicates
split search box into 4 boxes and push on stack
decrease stack pointer
top of stack?
N
Y
flag top sheet poles
S = success
F = failure
Y = yes
N = no

FIG. 8